Carbon and nutrient colimitations control the microbial response to fresh organic carbon inputs in soil at different depths

Lorène Siegwart, Gabin Piton, Christophe Jourdan, Clément Piel, Joana Sauze, Soh Sugihara, Isabelle Bertrand

Contents lists available at ScienceDirect

Geoderma

Carbon and nutrient colimitations control the microbial response to fresh organic carbon inputs in soil at different depths

Lorène Siegwart [a], Gabin Piton [a], Christophe Jourdan [a,b], Clément Piel [c], Joana Sauze [c], Soh Sugihara [d], Isabelle Bertrand [a,*]

[a] UMR Eco&Sols, Univ Montpellier, CIRAD, INRAE, IRD, InstitutAgro Montpellier, Montpellier, France
[b] CIRAD, UMR Eco&Sols, Montpellier F-34398, France
[c] ECOTRON Européen de Montpellier, UAR 3248 CNRS, 1 Chemin du Rioux, Montferrier sur Lez 34980, France
[d] Institute of Agriculture, Tokyo University of Agriculture and Technology, Tokyo, Japan

ARTICLE INFO

ABSTRACT

Despite the potential of subsoil carbon (C) to buffer or amplify climate change impacts, how fresh C and nutrients interact to control microorganismal effects on the C balance in deep soil horizons has yet to be determined. In this study, we aimed to estimate the impact of fresh C input at different soil depths on soil microbial activity. To conduct this study, Mediterranean soils from 3 layers (0–20, 20–50 and 50–100 cm of depth) were incubated over 28 days. Carbon and nutrient fluxes were measured after the addition of an amount of C equivalent to the postharvest root litter derived-C of a barley crop (4.3 atom% ^{13}C), with and without nitrogen and phosphorus supply. We found that the microbial mineralization was C limited in the topsoil, while C and N colimited in the subsoil. These variations in stoichiometric constraints along the soil profile induced different microbial responses to C and/or nutrient addition. A stronger priming effect was observed in the topsoil than in the subsoil, and the sole C addition induced a negative C balance. Conversely, subsoil showed a positive C balance following fresh C addition, changing to critical soil C losses when nutrients were supplied with C. Our results show that fresh C input to subsoil (e.g., through deep-rooting crops) might foster soil C sequestration, but this positive effect can be reversed if such C inputs are combined with high nutrient availability (e.g., through fertilization), alleviating microbial limitation at depth.

1. Introduction

Increasing root biomass at depth has been suggested as a lever to foster soil C (carbon) storage (Ojeda et al., 2018). In soil, the fates of litter-derived C and soil organic C depend on the microbial biomass, its metabolism and its resource acquisition strategy (Fontaine et al., 2007, Bernard et al., 2022). The CO_2 emissions from soil organic C decomposition following fresh organic matter (FOM) supply is the process called the priming effect (PE) (Kuzyakov et al., 2000; Fontaine et al., 2007; Bernard et al., 2022). In other words, PE is the effect of fresh organic matter addition on native organic matter mineralization changes, which can be enhanced (positive) or reduced (negative). While the impact of litter quality (Fanin et al., 2016; Lin et al., 2020; Liu et al., 2020b; Fanin et al., 2020) and soil properties (Perveen et al., 2019;

Bastida et al., 2019; Chen et al., 2019; Siles et al., 2022) on microbial mechanisms and especially PE have been widely studied in topsoil, the variations across depth gradients are still unclear (Rumpel et al., 2012; Jones et al., 2018; Moreira et al., 2022).

Subsoil properties exhibit many differences compared to topsoil properties (Sanaullah et al., 2011; Sanaullah et al., 2016; Button et al., 2022), partly due to the absence of soil plowing: more stable physico-chemical conditions (Holden and Fierer, 2005); lower availability of fresh plant material, i.e., root residues and C derived from rhizodeposition (Müller et al., 2016); lower organic C content (Blume et al., 2002); and lower C:N ratios (Rumpel and Kögel-Knabner, 2011). Deep soil organic matter is generally older than that in topsoil and is considered to have a greater degree of recalcitrance (Batjes, 1996). Vertical variations in C resources (plant litter and soil organic matter) can impact microbial

---

abundance and enzyme activity, which generally decrease with soil depth (Sanaullah et al., 2016; Piotrowska-Długosz et al., 2022b; Piotrowska-Długosz et al., 2022a) and are related to changes in microbial community composition and structure (Sanaullah et al., 2016). Microorganism physiological traits also respond to soil depth, with contrasting patterns reported for the microbial metabolic quotient (qCO$_2$) (Lavahun et al., 1996; Fang and Moncrieff, 2005), growth rate and C use efficiency (Spohn et al., 2016; Li et al., 2021a). C use efficiency is defined as the ratio of C assimilated to C respired and is a major factor for soil C storage (Cotrufo et al., 2013; Sinsabaugh et al., 2013; Kallenbach et al., 2019; Angers et al., 2022).

Because of the limited resources at depth, the stoichiometric response of soil microorganisms may govern the C and nutrient fluxes (Mooshammer et al., 2014b; Zechmeister-Boltenstern et al., 2015). For example, lower soil (i.e., resource for the microorganisms) C:N ratios in the cultivated subsoil (Batjes, 1996; Schneider et al., 2021) can lead to C limitations, to high C use efficiency and thus to high N mineralization fluxes (Mooshammer et al., 2014b; Zechmeister-Boltenstern et al., 2015). To highlight resource stoichiometric constraints, two complementary approaches can be used: the C:N imbalance (Karhu et al., 2022), reflecting microbial nutrient demand compared to resource availability (Li et al., 2021b), and the assessment of changes in enzyme C:N:P ratios, which are expected to reflect relative limitations of the soil microorganisms, as they generally invest preferentially in enzymes for the acquisition of the most limiting elements (Fanin et al., 2016; Cui et al., 2021), despite some limits to this approach (Mori, 2020).

Due to contrasting microbial properties and nutrient availability along the soil profile, the fate of FOM inputs can differ between top- and subsoil: faster root litter decomposition is observed in the topsoil (Pries et al., 2018; Siegwart et al., 2022a), and a lag phase due to slower development of soil microbial biomass seemed to prevail before decomposition in the subsoil (Sanaullah et al., 2011; Sanaullah et al., 2016). Differences in PE have also been reported between the topsoil and subsoil. The legacy of the carbon inputs has been shown to mediate the magnitude of PE (Schiedung et al., 2023). Further, few studies report an absence of PE in the subsoil in contrast to a significant positive PE in the topsoil from the same profile (Salomé et al., 2010; de Graaff et al., 2014), explaining these differences by the physical separation of the C-substrate (i.e., residue) and decomposers (Xiang et al., 2008; Salomé et al., 2010). In contrast, other studies have reported a high positive PE in subsoils (Fontaine et al., 2007; Karhu et al., 2016; Shahzad et al., 2019), justifying it by a strong C (energy) limitation. In other words, previous studies measuring PE at different soil depths find contrasting results, with a PE either higher or lower in the subsoil than in the topsoil. The differences between top- and subsoils are not always explained in these studies, because of lacking measurements of complementary variables. More specifically, microbial limitations for C or nutrients are great driver for soil organic C sensitivity to PE (Gaudel et al., 2021), and they could in fact explain the PE variations along a soil depth gradient. Two hypotheses have been proposed to explain such control of soil organic matter priming by soil nutrient availability: 'stoichiometric decomposition', when stoichiometric ratios of the inputs match those of the microbial demand (Chen et al., 2014), generally occurring in the first days (immediate PE) following the inputs (Razanamalala et al., 2018), and 'microbial N-mining' under N-shortage conditions (Craine et al., 2007), possibly occurring after the stoichiometric decomposition PE (Razanamalala et al., 2018). Despite the important consequences for C dynamics, most studies investigating the microbial response to FOM addition in subsoil (Fontaine et al., 2007; Salomé et al., 2010; de Graaff et al., 2014; Shahzad et al., 2019) do not take into account the soil and microbial nutrient status and stoichiometry.

Our study aims to assess the impact of soil nutrient availability on the microbial response to fresh organic C addition according to depth. To do so, we selected an arable soil with low organic C content (± 0.3 % at 0–20 cm depth) representative of the soils found in the Mediterranean climate (Ferreira et al., 2022; Siegwart et al., 2022b) to conduct incubations under controlled conditions. We hypothesized that soil microbial biomass and mineralization activities would be C-limited and more strongly limited in soils from the deeper horizons than in the topsoil. The addition of a small amount of C to these soils could overcome these limitations, especially at depth, while shifting microorganisms to nutrient limitations in both top- and subsoil, as the topsoil would be characterized by a high soil C:N ratio and the subsoil would have a small nutrient pool compared to the C amendments. The resulting nutrient limitations following C input would induce different microbial responses (enzymatic stoichiometry and PE) along the soil profile depending on the strength of the potential colimitations for C and nutrients assessed by a combined input of C and nutrients.

2. Materials and methods

2.1. Soil sampling

The soils were collected in the « Dispositif Instrumenté en Agroforesterie Méditerranéenne sous contrainte hydrique » (DIAMs) at the experimental station of INRAe (UE Diascope, Mauguio, France) in May 2021. The climate is Mediterranean, and the soils are classified as Skeletic Rhodic Luvisols (IUSS Working group WRB, 2014). The site is divided into three independent plots. In 2017, this site was transformed into an agroforestry system with "alley-cropping" as a plantation of black locust (*Robinia pseudoacacia*) with a density of 295 trees ha^{-1} (tree lines spaced 17 m apart). On the 22nd of January 2021, barley (*Hordeum vulgare*) was sown as a spring crop at a sowing density of 180 kg ha^{-1}. Fertilization campaigns were conducted with a Smart N 46 Fertilizer on the 4th of March 2021 (40 kg N ha^{-1}) and on the 26th of April 2021 (58.4 kg N ha^{-1}). Harvest occurred on June 30th, 2021, and straw was left on the soil surface.

According to previous studies conducted at the same site (Siegwart et al., 2022b), the soil properties did not vary according to the distance perpendicular to the tree, as this agroforestry system was young (trees planted in 2017). Consequently, this study focused on the inter row. In May 2021, corresponding to the flowering period of barley, 3 replicated pits (one on each independent plot) were dug in the middle of the inter row (1.7 m wide × 1.7 m long × 1.5 m deep), where no influence of the tree on microclimate was observed (e.g., no shadow). During the excavation of the pits, soil was sampled from the soil profile with a backhoe bucket from 3 layers, up to the maximum cereal rooting depth (0–20, 20–50 and 50–100 cm of depth), corresponding to the identified soil horizons in which crop roots had been previously found and quantified (Siegwart et al., 2022b). The soils were immediately sieved on a 2 mm sieve and stored at 4 °C prior to analysis. The soil physicochemical properties are summarized in Table 1. Among the most noteworthy characteristics, soil pH was ranging from 6.4 at 0–20 cm to 7.4 at 50–100 cm depth. While soil organic C, total N and total P significantly decreased with increasing depth, the stoichiometric ratios (C:N:P) did not vary between the 3 studied soil layers (p-value > 0.05, Table 1).

2.2. Experimental design

All soils (from 3 replicated pits × 3 soil layers) were incubated in 4 treatments representing different resource additions: Ctrl with water only, Glu with glucose (C), Nut with nutrients (N + P) and Glu + Nut with glucose + nutrients (C + N + P). The Glu treatment evaluated the microbial response to organic C addition to the soil and its control treatment was Ctrl, without C addition. The Glu + Nut treatment evaluated the microbial response to organic C addition to the soil in presence of nutrients, which were added simultaneously to overcome hypothetical microbial nutrient needs. Its control treatment was Nut, without C but with nutrient addition (Feng and Zhu, 2021).

[13]C-labelled glucose was used to mimic fresh C supply from plant roots. The quantity of added C was 70 mgC kg$_{soil}^{-1}$, which corresponded to the postharvest root litter-derived C inputs from barley assumed from

Table 1
Initial soil physicochemical properties according to depth (0–20, 20–50 and 50–100 cm). Data are mean values ± standard deviations (n = 3). Lowercase letters indicate significant differences between each soil depth (p value < 0.05).

	0–20 cm			20–50 cm			50–100 cm			Statistics
	Mean	Sd		Mean	Sd		Mean	Sd		p-value
Bulk density (g cm^{-3})	1.17	0.05	a	1.69	0.01	b	1.87	0.10	c	**7.88×10^{-15}**
Clay (g kg^{-1})	187.0	19.5	a	269.0	96.2	ab	458.3	94.7	b	**1.43×10^{-2}**
Silt (g kg^{-1})	326.7	13.5		315.0	21.6		273.3	77.2		0.30
Sand (g kg^{-1})	486.3	12.7	b	416.0	115.9	ab	268.3	30.9	a	**2.23×10^{-2}**
CEC	8.2	2.4	a	10.2	1.1	ab	17.6	4.6	b	**3.99×10^{-2}**
pH	6.4	0.4	a	7.0	0.6	ab	7.4	0.1	b	**2.22×10^{-2}**
Organic C (g kg^{-1})	11.3	3.0	b	8.5	1.6	ab	5.6	1.5	a	**1.97×10^{-2}**
CaCO$_3$ (g kg^{-1})	0.8	0.4		0.6	0.5		0.4	0.5		0.59
Total N (g kg^{-1})	0.9	0.2	b	0.7	0.1	ab	0.6	0.1	a	**4.58×10^{-2}**
Total P g kg^{-1}	0.6	0.2	b	0.5	0.2	ab	0.3	0.1	a	**3.59×10^{-2}**
C:N	12.7	2.5		12.8	0.5		9.8	3.1		0.28
C:P	20.4	0.4		18.5	3.2		16.3	3.5		0.24
N:P	1.6	0.4		1.4	0.2		1.7	0.2		0.48
16S:18S	0.98	0.42		1.40	0.85		2.75	1.48		0.16

the maximum root density (0.2 g$_{root}$ dm^{-3}) measured at the 0–20 cm depth in the same location as the soil sampling at barley's flowering stage (Siegwart et al., 2022b). The added C contained 4.3atom% excess 13C, as determined by isotopic mass spectrometry (Elemental Analyser Vario-PYROcube coupled to an IsoPrime Precision mass spectrometer, Elementar, UK). Solutions of KNO$_3$ and KH$_2$PO$_4$ were used as N and P additions, respectively. The quantities of added N and P were 20 mgN kg$_{soil}^{-1}$ and 10 mgP kg$_{soil}^{-1}$, respectively, which were calculated to sufficiently overcome a hypothetical microbial C:N ratio of 8 and a C:P ratio of 19 (Kirkby et al., 2011; Guillot et al., 2019), considering a hypothetical high C use efficiency of 80 % (Bernard et al., 2022).

For this study, independent replicates from 3 physically separated plots in the field were used to reflect the field heterogeneity.

A total of 216 soil closed plasma glass jars containing each 100 g of soil were prepared from the 3 field replicates (plots) × 3 soil layers (0–20, 20–50 and 50–100 cm) × 4 treatments (Ctrl, Glu, Nut and Glu + Nut) × 6 laboratory replicates (for sampling at days 0, 1, 3, 7, 14 and 28 after treatment starts). Before starting the treatments, the sieved soil samples were first preincubated for 2 weeks at 20 °C at 21 % of the water holding capacity, which was evaluated at 46.8±5.9 % (with no effect of the soil depth) with the funnel method (Bernard, 1963). At the end of the preincubation, all soils were mixed with their dedicated substrates (water, glucose, glucose + nutrients and nutrients for Ctrl, Glu, Glu + Nut and Nut respectively). Immediately after substrate addition, the soil moisture was adjusted and maintained throughout the incubation period to 32 % of the holding capacity mimicking the natural dry conditions of these Mediterranean soils. Disturbance induced by the mixing was thus similar between the controls (Ctrl and Nut) and the treatments (Glu and Glu + Nut). Our analyses then relied on the differences between the treatments and the associated control to disentangle the treatment effect from potential disturbance induced by the water/substrate addition. The incubation temperature was maintained at 20 °C. Then, destructive soil sampling occurred on days 0, 1, 3, 7, 14 and 28.

2.3. Carbon dynamics

On days 1, 3, 7, 10, 14, 17, 23 and 28, 50 μL of gas from the soil incubation jar was sampled through the septa with a 100 μL syringe (100F-LL-GT, SGE) and directly injected into 12 mL exetainers (Labco). For the jars without soils, 100 μL of gas was sampled. Those exetainers were previously flushed with N$_2$ (Alphagaz 2, Air Liquide). The CO$_2$ concentration and the isotopic ratios 13C/12C were measured with an isotope ratio mass spectrometer (IRMS, Delta V Plus, ThermoFisher Scientific, USA) equipped with a Gasbench II and a Conflo IV. The total C mineralization (C-CO$_2$ emissions) in Glu (and Glu + Nut) treatments was noted ^{Total}C-CO$_2$, and the C mineralization in the Ctrl (and Nut)

treatments was noted ^{Control}C-CO$_2$. The mineralization of C was reported per g of kg soil and per g of soil organic C. The isotopic excess in the labelled sampled was compared to that of the unlabelled soils for each fraction. The mineralization of C derived from the added glucose (^{NewlyfromaddedC}C-CO$_2$) was calculated from the released 13C-CO$_2$, considering the excess 13C of 4.3 atom% of the added C.

The contribution of carbonates to the C emissions was meant to be nonsignificant, as the CaCO$_3$ content was low (<1 g kg^{-1}) and independent of soil depth (Table 1).

At each date, soil layer and replicate, the PE was calculated in Glu and Glu + Nut as Fontaine et al. (2011):

$$PE = {}^{Total}C\text{-}CO_2 - {}^{NewlyfromaddedC}C\text{-}CO_2 - {}^{Control}C\text{-}CO_2$$

where ^{Total}C-CO$_2$ is the total C mineralization from the soils of treatment Glu (or Glu + Nut), ^{NewlyfromaddedC}C-CO$_2$ is the mineralized C derived from the added glucose, and ^{Control}C-CO$_2$ is the total C mineralization from the soils of treatment Ctrl (or Nut, respectively). All data were expressed as mgC kg$_{soil}^{-1}$.

On Day 28, the soils were analysed by isotopic mass spectrometry (Elemental Analyser Vario-PYROcube coupled to an IsoPrime Precision mass spectrometer, Elementar, UK) to determine the isotopic ratios 13C/12C and C contents. The isotopic excess was given by the difference between the sample and the standard reference PDB. The soil organic C derived from the added glucose (^{NewlyfromaddedC}SOC) was calculated from the measured soil 13C, considering the excess 13C as 4.3atom% of the added C.

At the end of the experiment for each soil layer and treatment, the change in soil organic C induced by the addition of glucose was calculated as Fontaine et al. (2011):

$$\Delta SOC = {}^{NewlyfromaddedC}SOC - PE$$

where ΔSOC is the change in soil organic C induced by the addition of glucose, ^{NewlyfromaddedC}SOC is the remaining soil organic C derived from the added glucose and PE is the priming effect. All data were expressed as mgC kg$_{soil}^{-1}$.

The percentage of added C that was recovered was calculated as Fanin et al. (2020):

$$Recovery = \frac{{}^{NewlyfromaddedC}C\text{-}CO_2 + {}^{NewlyfromaddedC}SOC}{{}^{added}C} \times 100$$

where *Recovery* is the percentage of added C that was recovered at the end of the experiment, ^{NewlyfromaddedC}C-CO$_2$ is the mineralized C derived from the added glucose, ^{NewlyfromaddedC}SOC is the remaining soil organic C derived from the added glucose and ^{added}C is the amount of added C. All

data were expressed as $mgC\,kg_{soil}^{-1}$, except Recovery as %.

2.4. Microbial biomass

On days 0, 1, 3, 7, 14 and 28, the microbial C and N biomass were evaluated with the chloroform fumigation-extraction method (Brookes et al., 1985; Vance et al., 1987a) immediately after soil sampling. Briefly, the soluble C and N were extracted with K_2SO_4 in fumigated and nonfumigated soils and determined with a TOC/TN analyser (TOC-VCSH/TNM-1, Shimadzu). The soluble C measured in the nonfumigated soils accounted for the soil dissolved organic C. The total microbial biomass C and N were calculated as the difference between the fumigated and the nonfumigated soils, corrected with a conversion factor of 0.45 (Vance et al., 1987a; Vance et al., 1987b). The total microbial biomass in the Glu (and Glu + Nut) treatments was noted $^{Total}MBC$, and the microbial biomass in the Ctrl (and Nut) treatments was noted $^{Control}MBC$. In addition, 10 mL subsamples of the K_2SO_4 extracts were lyophilized and analysed by isotopic mass spectrometry (Elemental Analyser Vario-PYROcube coupled to an IsoPrime Precision mass spectrometer, Elementar, UK) to determine the isotopic ratios $^{13}C/^{12}C$. The isotopic excess was given by the difference between the sample and the standard reference PDB. A mass balance equation was used to determine the ^{13}C values of the microbial biomass C (Marx et al., 2010):

$$IE_{MBC} = \frac{\left(IE_{C_f} \times C_f\right) - \left(IE_{C_{nf}} \times C_{nf}\right)}{C_f \times C_{nf}}$$

where IE_{MBC} is the isotopic excess of the microbial biomass C; IE_{C_f} and $IE_{C_{nf}}$ are the isotopic excess of the fumigated and nonfumigated samples, respectively; and C_f and C_{nf} are the quantities of C in the fumigated and nonfumigated K_2SO_4 extracts, respectively. The newly formed microbial biomass C derived from the added glucose ($^{NewlyfromaddedC}MBC$) was calculated from IE_{MBC}, considering the excess ^{13}C as 4.3 atom% of the added C.

At each date, soil layer and replicate, the newly formed microbial biomass derived from soil C rather than from the added glucose was calculated in Glu and Glu + Nut as Fanin et al. (2020):

$$^{NewlyfromaddedC}MBC = {}^{Total}MBC - {}^{NewlyfromaddedC}MBC - {}^{Control}MBC$$

where $^{NewlyfromaddedC}MBC$ is the newly formed microbial biomass derived from soil C in the soils of the Glu (or Glu + Nut) treatment, $^{Total}MBC$ is the total microbial biomass in the soils of the Glu (or Glu + Nut) treatment, $^{Control}MBC$ is the total microbial biomass in the soils of the Ctrl (or Nut) treatment and $^{NewlyfromaddedC}MBC$ is the newly formed microbial biomass derived from the added glucose in the soils of the Glu (or Glu + Nut) treatment. It is worth noting that the variable $^{Newly\,from\,soil\,C}MBC$ does not necessarily represent biomass associated with cells distinct to the $^{Newly\,from\,added\,C}MBC$. A single cell can increase its biomass using both added C glucose and native SOC, thus contributing to both variables. This does not interfere with the interpretation of this variable because we are interested in the general flow between microorganisms and CO_2 and not in its dispatching within the different microbial communities. All data were expressed as $mgC\,kg_{soil}^{-1}$.

The microbial imbalance ratio, defined as the $(C:N_{resource}):(C:N_{needs})$ ratio, was calculated for each soil layer, treatment and date as the C:N ratio of soil over the C:N ratio of the microbial biomass (Mooshammer et al., 2014b; Li et al., 2021b). A decreasing (or increasing) imbalance ratio potentially reflects an increasing N limitation (or C limitation, respectively) (Mooshammer et al., 2014a).

For each soil layer and replicate, the C use efficiency was calculated in the Glu and Glu + Nut treatments during the growing phase of the microorganisms, i.e., during the first day of the incubation as Sauvadet et al. (2018):

$$CUE = \frac{\Delta^{NewlyfromaddedC}MBC}{\Delta^{NewlyfromaddedC}MBC + {}^{NewlyfromaddedC}C\text{-}CO_2}$$

where *CUE* is the C use efficiency, $\Delta^{NewlyfromaddedC}MBC$ is the newly formed microbial biomass derived from the added glucose between Day 0 and Day 1, and $^{NewlyfromaddedC}C\text{-}CO_2$ is the mineralized C derived from the added glucose. All data were expressed as $mgC\,kg_{soil}^{-1}$, except the CUE in %.

2.5. Enzymatic activities

On days 1, 3, 7, 14 and 28, part of the sampled soils was immediately frozen at $-20\,^{\circ}C$ to measure the potential activities of 4 hydrolytic enzymes (Bell et al., 2013): β-1,4-glucosidase (BG), which hydrolyses cellulose (organic C); N-acetyl-glucosaminidase (NAG), which hydrolyses chitin and peptidoglycan; leucine aminopeptidase (LAP), which hydrolyses leucine and other hydrophobic amino acids from the N-terminus of polypeptides; and alkaline phosphatase (AP), which hydrolyses phosphosaccharides and phospholipids to produce phosphate ions (Sinsabaugh et al., 2008). The enzymatic activities ($nmol/g_{soil}\,min^{-1}$) were measured with a fluorometric microplate reader (Victor 3, Perkin Elmer, 365 nm excitation and 450 nm emission). C acquisition was represented by the activity of BG, and N acquisition was represented by the sum of the activities of NAG and LAP. P acquisition was represented by the activity of AP.

For each soil layer, treatment and date, ecoenzymatic stoichiometry was calculated as Fanin et al. (2016) and Cui et al. (2021) by plotting the relative proportion of C versus N acquiring activities (y) according to the relative proportion of C versus P acquiring enzyme activities (x). The vector lengths were calculated as the square root of the squared sum of x and y. The vector angles were calculated as the arctangent of the point (x, y).

2.6. Nutrient dynamics

On days 0, 1, 3, 7, 14 and 28, soil nutrient contents were measured immediately after sampling. Soil mineral N was extracted with a 1:4 soil-1 M KCl solution. NO_3^- and NH_4^+ were determined with a continuous flow analyser (San ++ Automated Wet Chemistry Analyser, Skalar), and the sum of NO_3^- and NH_4^+ accounted for the mineral soil N content. The soil available P content was also measured (Olsen, 1954). The net N mineralization was calculated as the difference between the mineral N content at a given sampling date and the value at Day 0 (Fanin et al., 2020).

2.7. Statistical analyses

Linear mixed models were used to analyse the effects of the soil layers, treatments, dates and their interactions as fixed factors and the three replicated profiles as random factors on all studied variables, except the cumulated ones. For the cumulated variables and for the variables not significantly affected by the date of sampling, linear mixed models were used by only testing the effect of the soil layers, treatments and their interaction as fixed factors and the three replicated profiles as random factors. Variables presenting significant differences on only a few dates were selected, and a model per date was applied. Post hoc Tukey tests were used to assess differences between soil depths and locations. The *lme4* and *car* packages were used for all the linear mixed models and analyses of variance. The normality of the residuals was verified with a Shapiro–Wilk test, and the homogeneity of the variances was verified with a Bartlett test. When necessary (p values < 5 %), logarithmic, square root, Box–Cox or Yeo Johnson transformations were applied. All statistical analyses were performed with R software (version 4.0.0).

3. Results

3.1. Carbon and nutrient mineralization

C mineralization and its response to glucose and nutrient addition changed along the soil profile. The C addition stimulated C mineralization with higher ^{Total}C-CO_2 (i.e., with C addition) than ^{Control}C-CO_2 (i. e., without C addition) in all the soil layers. Furthermore, when expressed as a proportion of soil organic C, ^{Total}C-CO_2 was significantly different in the 3 soil layers (p value $= 2.38 \times 10^{-5}$, Supplementary Table 1). In fact, the accumulated amount of ^{Total}C-CO_2 after 28 days was significantly lower in the subsoil than in the topsoil, ranging across treatments from 7 to 25 mgC-CO_2 g_{soilC}^{-1} at 50–100 cm compared to 20 to 40 mgC-CO_2 g_{soilC}^{-1} at 0–20 cm (Fig. 1a). As expected, in all the soil layers, the Glu and Glu + Nut treatments presented higher C mineralization than the Nut and Ctrl treatments (p value $= 8.47 \times 10^{-7}$, Supplementary Table 1). The increase in C mineralization following glucose addition tended to be greater in the subsoil ($\times 2$ at 50–100 cm) than in the topsoil ($\times 1.4$ at 0–20 cm). Similar trends were observed when expressing the mineralized total C per g of soil rather than per g of soil organic C (data not shown). Most of the total CO_2 was emitted in the first 3 days of incubation for all layers and treatments, including the controls (Supplementary Fig. 1). However, the subsoil at 50–100 cm presented relatively delayed CO_2 emissions compared to those in the upper soil layers (Fig. 1a). Furthermore, the metabolic quotient qCO_2 presented a significant increase at Day 3 only in the 0–20 and 20–50 cm layers with glucose addition (Supplementary Fig. 2).

In the glucose-amended treatments, additional CO_2 was not only emitted from the added C ($^{Newly\ from\ added\ C}$C-CO_2) but also from soil C (PE), mainly during the first 3 days of incubation (Fig. 2). The soils from 50 to 100 cm had significantly lower PE than the two other layers (p value $= 2.79 \times 10^{-8}$, Supplementary Table 2), and the Glu treatments had higher PE values than those of the Glu + Nut (p value $= 1.60 \times 10^{-2}$). However, these differences occurred only during the first days of incubation; then, the PE was equivalent between all layers and treatments.

The mineral N dynamics were also significantly impacted by soil layer and treatment (Supplementary Table 1). For all soil layers, the soils in the Ctrl treatment showed progressive net mineralization that was slower in the 50–100 cm layer than in the upper layers. Conversely, in the other treatments, a rapid immobilization of N (Fig. 1b) was observed with a decrease of the net N mineralization in the negatives in the first days of incubation (Fig. 1b). This immobilization was only slight in the Nut treatment, while representing approximately 7.5, 9 and 12 mgN kg_{soil}^{-1} for the layers at 0–20, 20–50 and 50–100 cm, respectively, in the Glu + Nut treatment. For this treatment, the peak of immobilization was reached at Day 14 except for the 20–50 cm soil layer, for which it was at Day 7. After this immobilization phase, important net mineralization occurred in the surface layer equally across all treatments (on average + 16.4±15.9 mgN kg_{soil}^{-1}) to reach a significantly higher N level in the Nut and Ctrl treatments than in the glucose-amended treatments (p value < 2.2×10^{-16}). In contrast, in comparison to the topsoil, the deepest soils presented lower remineralization (+1.5, +5.7 and +5.1 mgN kg_{soil}^{-1} in the Ctrl, Nut and Glu + Nut treatments, respectively) and even no remineralization in the Glu treatment, with a soil mineral N content stabilized at 0 mgN kg_{soil}^{-1} since Day 3 (Supplementary Fig. 3). This result highlighted a limitation in N in the subsoil amended with C only. No effect of nutrient addition was observed on the soil Olsen P (Supplementary Figs. 3 and 4).
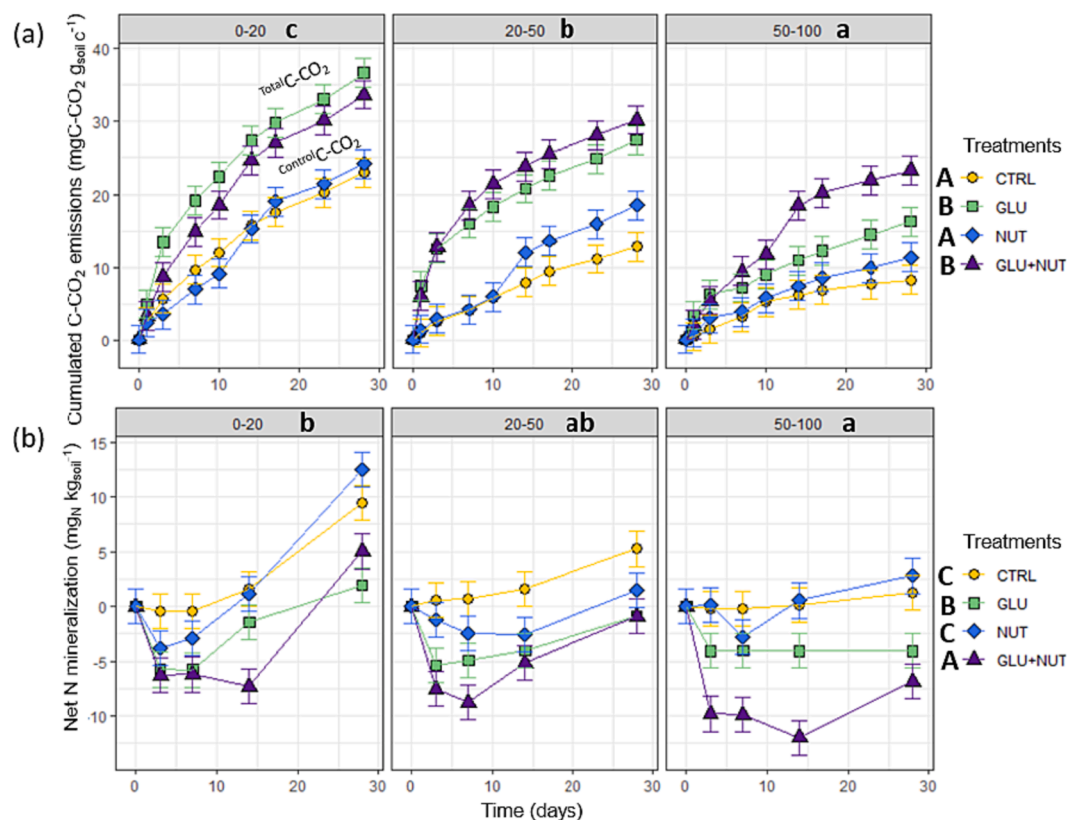

Fig. 1. Mineralization of C and N–cumulated ^{Total}C-CO_2 and ^{Control}C-CO_2 emissions normalized by the soil organic C content (a) and net N mineralization (b) according to time in the 3 soil layers (0–20, 20–50 and 50–100 cm) and for the 4 treatments (Ctrl: no addition, Glu: glucose addition, Nut: nutrient addition and Glu + Nut: glucose and nutrient addition). Data are mean values, and error bars represent the estimated standard errors from the mixed effect model (n = 3). For each graph (a – C mineralization and b – N mineralization), lowercase letters indicate significant differences between the soil layers, and uppercase letters indicate significant differences between the treatments.
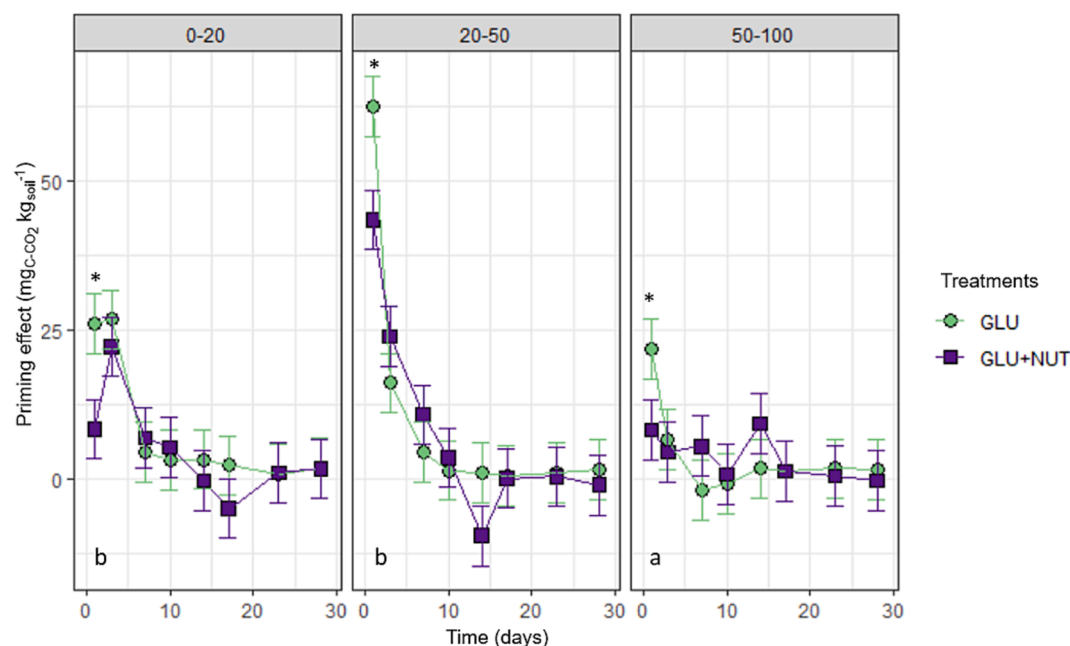
Fig. 2. Priming effect according to time in the 3 soil layers (0–20, 20–50 and 50–100 cm) and for the 2 treatments (Glu: glucose addition and Glu + Nut: glucose and nutrient addition). Data are mean values, and error bars represent the estimated standard errors from the mixed effect model (n = 3). * indicates that Glu was significantly higher than Glu + Nut. Lowercase letters indicate significant differences between the soil layers at Day 1 and Day 3.

3.2. Microbial biomass

On the first day of incubation, all C fractions contributing to the microbial biomass increased in all treatments and all soil layers (Fig. 3). Then, from Day 3 to Day 28, the ^{Control}MBC returned to its initial amount: approx. 150 mgC kg_{soil}^{-1} at 0–20 and 90 mgC kg_{soil}^{-1} at 50–100 cm,

the $^{Newly\ from\ soil\ C}$MBC was constant at approximately 30–40 mgC kg_{soil}^{-1}, and the $^{Newly\ from\ added\ C}$MBC was constant at approximately 3 mgC kg_{soil}^{-1}. Hence, the following description focuses on the microbial biomass evolution from Day 0 to Day 1:

On Day 1, without glucose addition, the Control MBC was significantly higher in the Nut treatment than in the Ctrl treatment (p value =
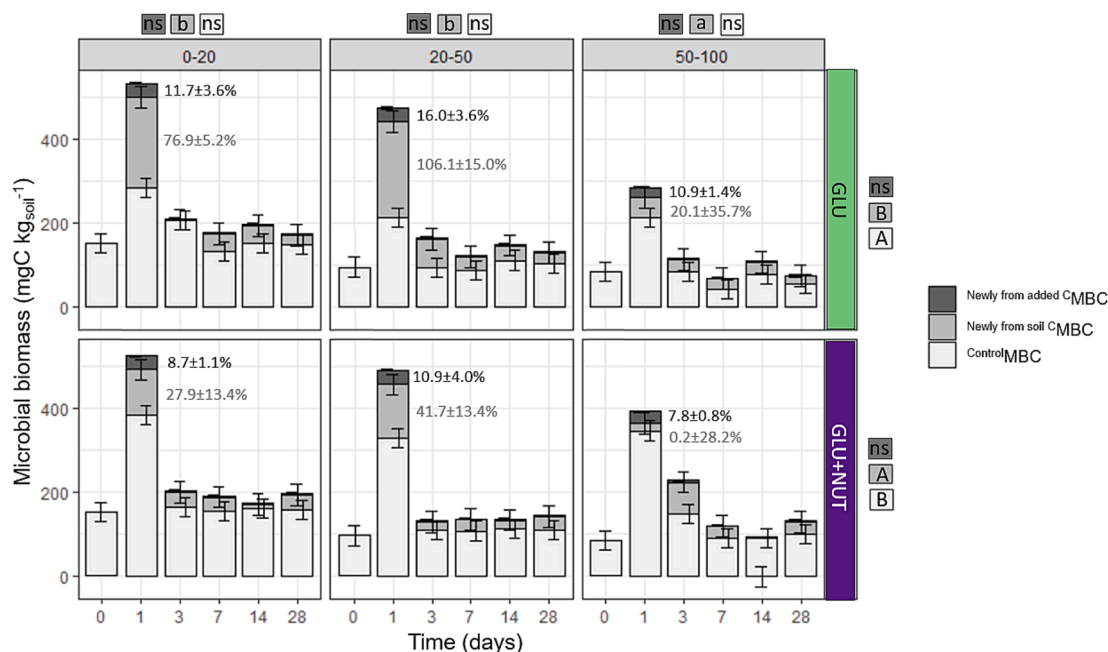

Fig. 3. Microbial biomass according to time in the 3 soil layers (0–20, 20–50 and 50–100 cm) and for the 2 treatments (Glu: glucose addition and Glu + Nut: glucose and nutrient addition). Colours accounted for the type of microbial biomass (black: $^{Newly\ from\ added\ C}$MBC – the newly formed microbial biomass derived from the added glucose, grey: $^{Newly\ from\ soil\ C}$MBC – the newly formed microbial biomass that was derived from soil C instead of from the added C, and white: ^{Control}MBC (in Ctrl for Glu and in Nut for Glu + Nut)). Data are mean values, and error bars represent the estimated standard errors from the mixed effect model (n = 3). For each type of biomass, lowercase letters indicate significant differences between the soil layers, uppercase letters indicate significant differences between the treatments at Day 1 only, and "ns" indicates "not significant". Numbers expressed in % represent the newly formed biomass (from added C and from soil C according to the font colour) calculated as a proportion of the biomass in the controls for each soil layer and treatment at Day 1.

7.61×10^{-3}, Supplementary Table 1), indicating that sole nutrient addition stimulated the acquisition of C from the soil organic C by the microbial biomass.

All treatments and soil layers accumulated similar amounts of [Newly from added C]MBC on Day 1 (p value = 0.57 and 0.09, respectively, Supplementary Table 1). However, the dissolved organic ^{13}C from the added ^{13}C glucose and remaining at Day 1, as an indicator of the unused C by the microorganisms, differed between soil layers (Supplementary Fig. 4). Little dissolved organic C from added C remained at 0–20 and 20–50 cm (approximately 20 and 10 mgC kg_{soil}^{-1}, respectively, in the Glu treatment), whereas at 50–100 cm, it was still at 62.5 ± 30.4 mgC kg_{soil}^{-1}, suggesting that all added C had been assimilated in the upper layers in the first hours of incubation but that 89 % of it was still in the dissolved organic C pool at Day 1 in the deeper layer.

The [Newly from soil C]MBC also differed between treatments and soil layers on Day 1. It was significantly higher in the Glu treatment than in the Glu + Nut treatment (p value = 1.39×10^{-2}, Supplementary Table 1) and significantly lower at 50–100 cm than in the upper soil layers (p value = 2.48×10^{-3}, Supplementary Table 1). In addition, a lag phase was observed at the 50–100 cm depth in the Glu + Nut treatment with higher [Newly from soil C]MBC at Day 3 than at Day 1.

The microbial biomass N showed extremely similar patterns to the total MBC and was higher in the upper soil layers than in the deeper soil layers (p value = 1.29×10^{-9}, Supplementary Table 1), and it increased with glucose addition (p value = 5.89×10^{-4}, Supplementary Table 1). However, it remained unchanged with the sole nutrient addition (data not shown).

The C use efficiency was high for all incubated soils, ranging from approximately 0.80 to 0.95 (Fig. 4). There was only a marginal difference (not significant) between treatments (p value = 0.13, Supplementary Table 1), with the Glu + Nut treatment mean higher than the Glu treatment mean in all soil layers.

The (C:$N_{resource}$):(C:N_{needs}) ratio indicated the availability of the resources relative to the microbial needs (Fig. 5). At depths of 0–20 cm for all treatments, this ratio was lower than 1 (below 0.17), showing a strong imbalance and, more specifically, a general C limitation. In the two other soil layers, while it was constantly low in the Ctrl, Nut and Glu + Nut treatments, the imbalance ratio was substantially increased by the sole glucose addition at the 20–50 and 50–100 depths. In the Glu treatment, the imbalance ratio was approx. = 1 at 20–50 cm of depth, in spite of strong temporal variations, suggesting a more balanced stoichiometry between the resources compared to microbial biomass compared to the 2 other layers. It was even higher at 50–100 cm (2.5 at
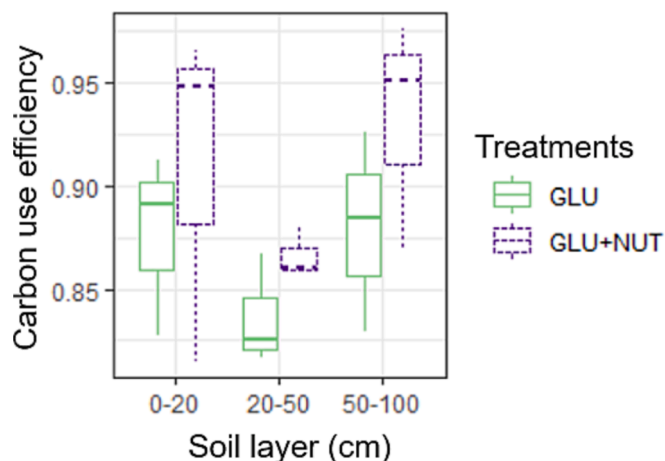

Fig. 5. Microbial imbalance ratio as the (C:$N_{resource}$):(C:N_{needs}) ratio according to time in the 3 soil layers (0–20, 20–50 and 50–100 cm) and for the 4 treatments (Ctrl: no addition, Glu: glucose addition, Nut: nutrients addition and Glu + Nut: glucose and nutrients addition). Data are mean values, and error bars represent the estimated standard errors from the mixed effect model (n = 3). * indicates the only significantly different soil layer within all treatments and the only significantly different treatment within all soil layers.

Day 13 and reaching very high values from Day 14), suggesting that the Glu treatment at 50–100 cm depth became nutrient limited (Fig. 5). The variations in the imbalance ratio were strongly related to the resources (soil C:N) more than to the needs because at the 50–100 cm depth, the microbial C:N was the same in the treatment Glu as in the other treatments in the same soil layer (Supplementary Fig. 5).

3.3. Enzymatic activity

The ecoenzymatic stoichiometry showed different relative C:N:P acquisitions according to soil layer and treatment (Supplementary Fig. 6a). While the ecoenzymatic stoichiometry showed equivalent vector angles in all the soil layers (p value = 0.94) and treatments (p value = 0.47, data not shown), the vector length was significantly impacted by the combined effect of soil layer and treatment (p value = 3.50×10^{-5}, Supplementary Table 1). In fact, the vector length decreased with increasing depth for all treatments, suggesting a lower C limitation in the deeper soil layers than in the upper ones. This result was in agreement with the decreasing enzymatic C:N ratio with increasing depth (Supplementary Fig. 8) due to lower C- and higher N-enzyme specific activities at 50–100 cm than at 0–20 cm (Supplementary Fig. 7). Furthermore, the vector length at 50–100 cm was significantly higher in the Glu + Nut treatment than in the other treatments, suggesting a decrease in nutrient limitation or an increase in C limitation (Supplementary Fig. 6b).

3.4. Carbon balance

At the end of the incubation experiment, the distribution of the added C in the different pools differed in the soils according to soil layer and treatment, despite equivalent C addition (Table 2). After 28 days, from 70.28 mgC kg_{soil}^{-1} of added C, 4.1, 2.6 and 1.3 % were still in the microbial biomass ([Newly from added C]MBC), while 14.2, 12.8 and 8.5 % were emitted as CO_2 ([Newly from added C]C-CO_2) at depths of 0–20, 20–50 and 50–100 cm, respectively. These fluxes were slightly higher when nutrients were added with C, although the difference was not significant. Furthermore, the remaining C that had not been emitted or immobilized in the microbial biomass C after 28 days (approx. 90 %) remained in the soil ([Newly from added C]SOC).

After 28 days of incubation, the cumulated PE was twice the amount

Fig. 4. C use efficiency during the growing phase of the microorganisms, i.e., during the first day of incubation (CUE) in the 3 soil layers (0–20, 20–50 and 50–100 cm) and for the 2 treatments (Glu: glucose addition and Glu + Nut: glucose and nutrient addition) (n = 3).
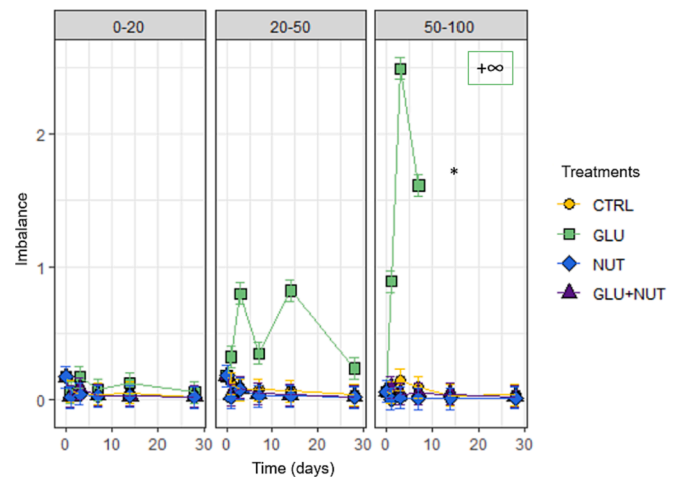
Table 2

C balance of the added C after 28 days of incubation in the 3 soil layers (0–20, 20–50 and 50–100 cm) and for the 2 treatments (Glu: glucose addition and Glu + Nut: glucose and nutrient addition). Data are mean values ± standard deviations. $^{NewlyfromaddedC}SOC$ is the remaining soil organic C derived from the added glucose, $^{NewlyfromaddedC}DOC$ is the remaining dissolved organic C derived from the added glucose, $^{NewlyfromaddedC}MBC$ is the newly formed microbial biomass derived from the added glucose, $^{NewlyfromaddedC}C\_CO_2$ is the mineralized C derived from the added glucose, PE is the priming effect, ΔSOC is the change in soil organic C induced by the addition of glucose, and *Recovery* is the percentage of added C that was recovered at the end of the experiment.

Soil layer	Treatment	Newly from added C_{SOC}	Newly from added C_{DOC}	Newly from added C_{MBC}	Newly from added C_{C-CO2}	PE	ΔSOC	Recovery
cm		mgC kg$_{soil}^{-1}$	mgC kg$_{soil}^{-1}$	mgC kg$_{soil}^{-1}$	mgC kg$_{soil}^{-1}$	mgC kg$_{soil}^{-1}$	mgC kg$_{soil}^{-1}$	% added C
0–20	Glu	66.2±9.7	0.9±0.9	2.9±0.5	10.4±3.6	141.9±36.6	−75.8 ± 46.7	109
	Glu + Nut	68.4±13.8	0.5±0.9	3.8±0.8	10.8±4.7	95.1±80.5	−26.6 ± 85.7	113
20–50	Glu	69.9±3.0	0.1±0.1	1.8±0.6	9.2±1.4	137.8±40.9	−67.4 ± 40.1	113
	Glu + Nut	68.7±5.1	2.0±3.2	2.0±1.2	13.0±5.4	105.0±87.2	−36.3 ± 83.1	116
50–100	Glu	69.7±4.6	0.6±0.1	0.9±0.8	6.0±2.6	54.9±40.7	5.5 ± 54.9	108
	Glu + Nut	69.9±12.9	0.3±0.3	2.1±1.1	6.2±1.2	84.8±44.5	−15.1 ± 46.8	108

of added C at 0–20 and 20–50 cm. Conversely, at 50–100 cm, the PE was 15 mgC kg$_{soil}^{-1}$ lower than the amount of added C (Table 2). When nutrients were added in addition to glucose, the PE was lower than that without nutrients in the upper soil layers, whereas at 50–100 cm, the PE was higher than that without nutrients (Supplementary Fig. 9a) and substantially higher than that in the other soil layers when reporting on a per soil organic carbon basis (Supplementary Fig. 9b). The high standard deviations of the PE led to high uncertainties in the calculated C balance ΔSOC.

4. Discussion

4.1. C and nutrient limitations of soil microorganisms at different depths

To test the first hypothesis that the microorganisms of the typical Mediterranean arable soil used in this study were C-limited, we added glucose to soil sampled from 3 different layers up to the maximum crop rooting depth (Siegwart et al., 2022b). The amount of added C was small compared to that in other studies testing priming effects with glucose addition (Tian et al., 2016; Karhu et al., 2016; Jia et al., 2017). However, the amount in our study was selected to represent the annual root litter-derived C input of a barley crop at the 0–20 cm depth cultivated in the same soil (Siegwart et al., 2022b). Glucose represents one of the dominant molecules exuded by roots and it is also used by soil microorganisms during root polysaccharide decomposition (e.g., cellulose). It thus represent a relevant model molecule to evaluate the microbial response to root C input (Kuzyakov, 2010; Gunina and Kuzyakov, 2015; Soong et al., 2020). Nevertheless, we are aware that organic molecules released by roots (rhizodepozition or decomposition) are very diverse and can differ from glucose in terms of stoichiometry and molecular complexity. And yet, the substrate's stoichiometry would drive PE more than its complexity (litter vs. soluble organic matter) according to a recent *meta*-analysis (Huo et al., 2022), underlining the interest of the present study. However, some studies still report different PE depending on the type of substrate (Hamer and Marschner, 2005; Di Lonardo et al., 2017; Heitkötter et al., 2017), with variable effects that call for more study using labelled root litters or different molecules to determine the underlying mechanisms and fully take into account the complex effect of root C input.

The amount of added C in our study stimulated the microbial biomass and activity (respiration and extracellular enzymes) in all soil layers in the short term i.e., the first days of incubation, confirming a C limitation. The C limitation across different depths was consistent with the low $(C:N_{resource}):(C:N_{needs})$ ratio observed in these soils, indicating an imbalance between the stoichiometry of the resources and of the microbial needs (Mooshammer et al., 2014b; Song et al., 2020). Such C limitation of soil microbial communities has been extensively reported across topsoil (Cheng et al., 1996; Demoling et al., 2007; Kallenbach and Grandy, 2011; Ning et al., 2021), but it has remained rarely investigated in deeper soil layers (Jones et al., 2018; Button et al., 2022).

In the present study, the response to C addition differed according to soil depth. In the topsoil, the addition of C resulted in a significant increase in microbial respiration (+152 and +106 mgC kg$_{soil}^{-1}$ in the Glu and Glu + Nut treatments, respectively) and biomass C (+249 and +140 mgC kg$_{soil}^{-1}$) compared to that in the control treatments. However, the stoichiometric imbalance ratio was constant because of significant microbial immobilization of N (+7.5 and +3.5 mgN kg$_{soil}^{-1}$ in the Glu and Glu + Nut treatments, respectively) driven by the addition of C. Therefore, N was not limiting in the topsoil, which could have been due to chemical fertilization practices during crop cultivation.

We found several evidence that subsoils can be colimited by C and nutrients. An equivalent quantity of added C was responsible for a lower increase in the CO$_2$ emissions (+61 mgC kg$_{soil}^{-1}$) in the subsoil than that in the topsoil. Despite the uncertainty of the ecoenzymatic stoichiometry analyses (Mori, 2020) and more particularly when applied to short term responses (Moorhead et al., 2023), the limitation patterns described above were in accordance with a smaller enzymatic vector, suggesting lower needs for C, in the subsoil than in the topsoil. When reported on a per soil organic C basis, the increase in total CO$_2$ emissions after C addition was similar at 50–100 cm (+1.1 %) to that at 0–20 cm (+1.3 %). Furthermore, the lower enzymatic C:N ratio and the higher N-acquisition specific activity in the subsoil compared to those in topsoil suggested that microorganisms at depth were more accustomed to facing nutrient limitation than topsoil communities (Fanin et al., 2016). Additionally, the addition of C in the subsoil extensively increased the stoichiometric imbalance ratio, as no N was available from day 3, suggesting a colimitation in C and nutrients in the subsoil. The colimitation of C and N following C addition in the subsoil was confirmed by the treatments with both C and nutrient addition, in which the subsoil showed higher production of microbial biomass C (+300 vs. + 200 mgC kg$_{soil}^{-1}$ from Day 0 to Day 1) and a higher respiration compared to those with C addition without nutrients. A longer enzymatic vector observed in the subsoil amended with C and nutrients compared to with C only was also consistent with the idea that nutrient limitation was relaxed (compared to C limitations that were strengthened) when C and nutrients were added together. Consequently, long term adjustment of the decomposer resource acquisition strategy to the stoichiometric constrains of their polymerized resource, as recently discussed by Moorhead et al. (2023), were consistent with the microbial biomass and activity response to resource pulse in our study. Such colimitations have also been reported in deep soils from tropical forests (Meyer et al., 2018; Liu et al., 2020a) and from temperate arable lands (Peixoto et al., 2021) but were contrary to our hypotheses based on the variations in the soil C:N ratio (Mooshammer et al., 2014b; Zhao et al., 2021), suggesting that the soil C:N ratio alone is not enough for predicting microbial mechanisms. Altogether, the results of this study showed that soil microbial limitations can change along the soil profile and confirmed that stoichiometric imbalance and, to a lesser extent, enzymatic stoichiometry in addition to nutrients fluxes, provide a better picture of these limitations than the soil stoichiometric ratio alone (Karhu et al., 2022).

4.2. Consequences of the C and nutrient colimitations on the fate of added C according to depth

The C addition stimulated the microbial metabolism, which induced a PE varying according to the stoichiometric constraints along the soil profile. First, after glucose addition, the mineralization of soil organic matter increased, and the soil organic matter was assimilated into microbial biomass, as the unlabelled microbial biomass increased. Our data thus suggested a 'real' PE more than an 'apparent' PE after glucose addition (Wu et al., 1993; Fontaine et al., 2004; Fanin et al., 2020). Furthermore, differences in intensity and temporal dynamics were observed between the top- and subsoil PE. In the subsoil layer (50–100 cm), the cumulative PE was lower (representing 1/3) than that in the topsoil (0–20 cm) after 28 days of incubation, consistent with previous findings (de Graaff et al., 2014). In addition to the lower intensity of PE in the subsoil, a lag in microbial response to C addition was found in the subsoil and has already been reported (Sanaullah et al., 2011; Sanaullah et al., 2016). Several hypotheses can explain the observed lag in the subsoil: (i) a higher proportion of microbial communities with slower growth rates, (ii) a higher proportion of dormant biomass (Maharjan et al., 2017; Joergensen and Wichern, 2018), (iii) the legacy of the C inputs (Schiedung et al., 2023) such as limited organic matter inputs and a resulting higher proportion of recalcitrant organic matter (stable C) (Fanin et al., 2020), or (iv) a shift from a stoichiometric decomposition PE to a N-mining PE due to the induced N limitations (Razanamalala et al., 2018). These differences contributed to the negative C balance in the topsoil and a positive C balance in the subsoil when comparing PE loss and added soil organic C. When nutrients were added with C, the C balance became negative in the subsoil, as opposed to our hypothesis based on the low soil C:N and in agreement with Meyer et al. (2018). These indicators suggested that the PE in the subsoil was consistent with the stoichiometric decomposition theory (Chen et al., 2014) with a PE explained by the stimulation of microbial metabolism induced by the relaxation of its stoichiometric constraints. In contrast, in the topsoil, the combined addition of C and nutrients reduced the PE compared to C addition alone. This was probably due to a positive effect of N on the C use efficiency, as already described by Manzoni et al. (2012), stimulating microbial biomass production instead of mineralization (Sinsabaugh et al., 2013). Then, the microbial biomass stabilized through the entombing effect (Liang, 2020), thus contributing to a relatively stable soil organic C pool and reducing the PE. Such reasoning was also involved in a recent study (Liao et al., 2022). However, in the present study, the reduction in PE in the topsoil when nutrients were supplied was not sufficient to shift the balance from negative to positive. Overall, a quantity of added C equivalent to in situ barley root input induced a PE, which was controlled by stoichiometric constraints on microbial metabolism and varied along the soil profile.

5. Conclusion

Our study showed that variations in stoichiometric constraints along a Mediterranean soil profile highly controlled the microbial response to a fresh C input (glucose) and the resulting C balance. Our results suggest that the priming effect induced by a fresh soluble C input into Mediterranean topsoil could be radically changed by increasing nutrient availability. By contrast to topsoil, subsoil microorganisms would be less reactive to fresh soluble C inputs, unless nutrient availability meets the microbial needs. The time lag showed by the subsoil stress the need of long incubations to detect the full subsoil response. Such studies would emphasize that the C balance resulting from farming practices, that increase fresh C input in subsoil (e.g., deep-rooted crops) could be highly linked with nutrient availability and associated practices (e.g., fertilization).

Authors' contributions

The study was conceived and designed by IB, SS and LS. Data collection was performed by LS, JS and CP. Data analysis was performed by LS. The first draft of the manuscript was written by LS, and all authors commented on previous versions of the manuscript. All authors read and approved the final manuscript.

Declaration of competing interest

The authors declare the following financial interests/personal relationships which may be considered as potential competing interests: Isabelle Bertrand reports financial support was provided by French National Institute for Agricultural Research INRAE.

Data availability

Data will be made available on request.

Appendix A. Supplementary data

Supplementary data to this article can be found online at https://doi.org/10.1016/j.geoderma.2023.116729.

References

Angers, D., Arrouays, D., Cardinael, R., Chenu, C., Corbeels, M., Demenois, J., Farrell, M., Martin, M., Minasny, B., Recous, S., Six, J., 2022. A well-established fact: Rapid mineralization of organic inputs is an important factor for soil carbon sequestration. Eur J Soil Sci. https://doi.org/10.1111/ejss.13242.

Bastida, F., García, C., Fierer, N., Eldridge, D.J., Bowker, M.A., Abades, S., Alfaro, F.D., Asefaw Berhe, A., Cutler, N.A., Gallardo, A., García-Velázquez, L., Hart, S.C., Hayes, P.E., Hernández, T., Hseu, Z.-Y., Jehmlich, N., Kirchmair, M., Lambers, H., Neuhauser, S., Peña-Ramírez, V.M., Pérez, C.A., Reed, S.C., Santos, F., Siebe, C., Sullivan, B.W., Trivedi, P., Vera, A., Williams, M.A., Luis Moreno, J., Delgado-Baquerizo, M., 2019. Global ecological predictors of the soil priming effect. Nat Commun 10, 3481. https://doi.org/10.1038/s41467-019-11472-7.

Batjes, N., h., 1996. Total carbon and nitrogen in the soils of the world. Eur J Soil Sci 47, 151–163. https://doi.org/10.1111/j.1365-2389.1996.tb01386.x.

Bell, C.W., Fricks, B.E., Rocca, J.D., Steinweg, J.M., McMahon, S.K., Wallenstein, M.D., 2013. High-throughput Fluorometric Measurement of Potential Soil Extracellular Enzyme Activities. JoVE J vis Exp e50961. https://doi.org/10.3791/50961.

Bernard, J.M., 1963. Forest Floor Moisture Capacity of the New Jersey Pine Barrens. Ecology 44, 574–576. https://doi.org/10.2307/1932538.

Bernard, L., Basile-Doelsch, I., Derrien, D., Fanin, N., Fontaine, S., Guenet, B., Karimi, B., Marsden, C., Maron, P.-A., 2022. Advancing the mechanistic understanding of the priming effect on soil organic matter mineralisation. Funct Ecol 36, 1355–1377. https://doi.org/10.1111/1365-2435.14038.

Blume, E., Bischoff, M., Reichert, J.M., Moorman, T., Konopka, A., Turco, R.F., 2002. Surface and subsurface microbial biomass, community structure and metabolic activity as a function of soil depth and season. Appl Soil Ecol 20, 171–181. https://doi.org/10.1016/S0929-1393(02)00025-2.

Brookes, P.C., Landman, A., Pruden, G., Jenkinson, D.S., 1985. Chloroform fumigation and the release of soil nitrogen: A rapid direct extraction method to measure microbial biomass nitrogen in soil. Soil Biol Biochem 17, 837–842. https://doi.org/10.1016/0038-0717(85)90144-0.

Button, E.S., Pett-Ridge, J., Murphy, D.V., Kuzyakov, Y., Chadwick, D.R., Jones, D.L., 2022. Deep-C storage: Biological, chemical and physical strategies to enhance carbon stocks in agricultural subsoils. Soil Biol Biochem 170, 108697. https://doi.org/10.1016/j.soilbio.2022.108697.

Chen, L., Liu, L., Qin, S., Yang, G., Fang, K., Zhu, B., Kuzyakov, Y., Chen, P., Xu, Y., Yang, Y., 2019. Regulation of priming effect by soil organic matter stability over a broad geographic scale. Nat Commun 10, 1–10. https://doi.org/10.1038/s41467-019-13119-z.

Chen, R., Senbayram, M., Blagodatsky, S., Myachina, O., Dittert, K., Lin, X., Blagodatskaya, E., Kuzyakov, Y., 2014. Soil C and N availability determine the priming effect: microbial N mining and stoichiometric decomposition theories. Glob Change Biol 20, 2356–2367. https://doi.org/10.1111/gcb.12475.

Cheng, W., Zhang, Q., Coleman, D.C., Ronald Carroll, C., Hoffman, C.A., 1996. Is available carbon limiting microbial respiration in the rhizosphere? Soil Biol Biochem 28, 1283–1288. https://doi.org/10.1016/S0038-0717(96)00138-1.

Cotrufo, M.F., Wallenstein, M.D., Boot, C.M., Denef, K., Paul, E., 2013. The Microbial Efficiency-Matrix Stabilization (MEMS) framework integrates plant litter decomposition with soil organic matter stabilization: do labile plant inputs form stable soil organic matter? Glob Change Biol 19, 988–995. https://doi.org/10.1111/gcb.12113.

Craine, J.M., Morrow, C., Fierer, N., 2007. Microbial Nitrogen Limitation Increases Decomposition. Ecology 88, 2105–2113. https://doi.org/10.1890/06-1847.1.

Cui, Y., Moorhead, D.L., Guo, X., Peng, S., Wang, Y., Zhang, X., Fang, L., 2021. Stoichiometric models of microbial metabolic limitation in soil systems. Glob Ecol Biogeogr 30, 2297–2311. https://doi.org/10.1111/geb.13378.

de Graaff, M.-A., Jastrow, J.D., Gillette, S., Johns, A., Wullschleger, S.D., 2014. Differential priming of soil carbon driven by soil depth and root impacts on carbon availability. Soil Biol Biochem 69, 147–156. https://doi.org/10.1016/j.soilbio.2013.10.047.

Demoling, F., Figueroa, D., Bååth, E., 2007. Comparison of factors limiting bacterial growth in different soils. Soil Biol Biochem 39, 2485–2495. https://doi.org/10.1016/j.soilbio.2007.05.002.

Di Lonardo, D.P., De Boer, W., Klein Gunnewiek, P.J.A., Hannula, S.E., Van der Wal, A., 2017. Priming of soil organic matter: Chemical structure of added compounds is more important than the energy content. Soil Biol Biochem 108, 41–54. https://doi.org/10.1016/j.soilbio.2017.01.017.

Fang, C., Moncrieff, J.B., 2005. The variation of soil microbial respiration with depth in relation to soil carbon composition. Plant Soil 268, 243–253. https://doi.org/10.1007/s11104-004-0278-4.

Fanin, N., Moorhead, D., Bertrand, I., 2016. Eco-enzymatic stoichiometry and enzymatic vectors reveal differential C, N, P dynamics in decaying litter along a land-use gradient. Biogeochemistry 129, 21–36. https://doi.org/10.1007/s10533-016-0217-5.

Fanin, N., Alavoine, G., Bertrand, I., 2020. Temporal dynamics of litter quality, soil properties and microbial strategies as main drivers of the priming effect. Geoderma 377, 114576. https://doi.org/10.1016/j.geoderma.2020.114576.

Feng, J., Zhu, B., 2021. Does calculation method affect the nutrient-addition effect on priming? Geoderma 393, 115040. https://doi.org/10.1016/j.geoderma.2021.115040.

Ferreira, C.S.S., Seifollahi-Aghmiuni, S., Destouni, G., Ghajarnia, N., Kalantari, Z., 2022. Soil degradation in the European Mediterranean region: Processes, status and consequences. Sci Total Environ 805, 150106. https://doi.org/10.1016/j.scitotenv.2021.150106.

Fontaine, S., Bardoux, G., Abbadie, L., Mariotti, A., 2004. Carbon input to soil may decrease soil carbon content. Ecol Lett 7, 314–320. https://doi.org/10.1111/j.1461-0248.2004.00579.x.

Fontaine, S., Barot, S., Barré, P., Bdioui, N., Mary, B., Rumpel, C., 2007. Stability of organic carbon in deep soil layers controlled by fresh carbon supply. Nature 450, 277–280. https://doi.org/10.1038/nature06275.

Fontaine, S., Henault, C., Aamor, A., Bdioui, N., Bloor, J.M.G., Maire, V., Mary, B., Revaillot, S., Maron, P.A., 2011. Fungi mediate long term sequestration of carbon and nitrogen in soil through their priming effect. Soil Biol Biochem 43, 86–96. https://doi.org/10.1016/j.soilbio.2010.09.017.

Gaudel, G., Poudel, M., Mosongo, P.S., Xing, L., Oljira, A.M., Zhang, Y., Bizimana, F., Liu, B., Wang, Y., Dong, W., Uwamungu, J.Y., Hu, C., 2021. Meta-analysis of the priming effect on native soil organic carbon in response to glucose amendment across soil depths. Plant Soil. https://doi.org/10.1007/s11104-021-05168-5.

Guillot, E., Hinsinger, P., Dufour, L., Roy, J., Bertrand, I., 2019. With or without trees: Resistance and resilience of soil microbial communities to drought and heat stress in a Mediterranean agroforestry system. Soil Biol Biochem 129, 122–135. https://doi.org/10.1016/j.soilbio.2018.11.011.

Gunina, A., Kuzyakov, Y., 2015. Sugars in soil and sweets for microorganisms: Review of origin, content, composition and fate. Soil Biol Biochem 90, 87–100. https://doi.org/10.1016/j.soilbio.2015.07.021.

Hamer, U., Marschner, B., 2005. Priming effects in different soil types induced by fructose, alanine, oxalic acid and catechol additions. Soil Biol Biochem 37, 445–454. https://doi.org/10.1016/j.soilbio.2004.07.037.

Heitkötter, J., Heinze, S., Marschner, B., 2017. Relevance of substrate quality and nutrients for microbial C-turnover in top- and subsoil of a Dystric Cambisol. Geoderma 302, 89–99. https://doi.org/10.1016/j.geoderma.2017.04.029.

Holden, P.A., Fierer, N., 2005. Microbial Processes in the Vadose Zone. Vadose Zone J 4, 1–21. https://doi.org/10.2136/vzj2005.0001.

Huo, C., Liang, J., Zhang, W., Wang, P., Cheng, W., 2022. Priming effect and its regulating factors for fast and slow soil organic carbon pools: A meta-analysis. Pedosphere 32, 140–148. https://doi.org/10.1016/S1002-0160(21)60064-4.

IUSS Working group WRB, 2014. World reference base for soil resources 2014: international soil classification system for naming soils and creating legends for soil maps. FAO, Rome.

Jia, J., Feng, X., He, J.-S., He, H., Lin, L., Liu, Z., 2017. Comparing microbial carbon sequestration and priming in the subsoil versus topsoil of a Qinghai-Tibetan alpine grassland. Soil Biol Biochem 104, 141–151. https://doi.org/10.1016/j.soilbio.2016.10.018.

Joergensen, R.G., Wichern, F., 2018. Alive and kicking: Why dormant soil microorganisms matter. Soil Biol Biochem 116, 419–430. https://doi.org/10.1016/j.soilbio.2017.10.022.

Jones, D.L., Magthab, E.A., Gleeson, D.B., Hill, P.W., Sánchez-Rodríguez, A.R., Roberts, P., Ge, T., Murphy, D.V., 2018. Microbial competition for nitrogen and carbon is as intense in the subsoil as in the topsoil. Soil Biol Biochem 117, 72–82. https://doi.org/10.1016/j.soilbio.2017.10.024.

Kallenbach, C., Grandy, A.S., 2011. Controls over soil microbial biomass responses to carbon amendments in agricultural systems: A meta-analysis. Agric Ecosyst Environ 144, 241–252. https://doi.org/10.1016/j.agee.2011.08.020.

Kallenbach, C.M., Wallenstein, M.D., Schipanksi, M.E., Grandy, A.S., 2019. Managing Agroecosystems for Soil Microbial Carbon Use Efficiency: Ecological Unknowns, Potential Outcomes, and a Path Forward. Front Microbiol 10.

Karhu, K., Hilasvuori, E., Fritze, H., Biasi, C., Nykänen, H., Liski, J., Vanhala, P., Heinonsalo, J., Pumpanen, J., 2016. Priming effect increases with depth in a boreal forest soil. Soil Biol Biochem 99, 104–107. https://doi.org/10.1016/j.soilbio.2016.05.001.

Karhu, K., Alaei, S., Li, J., Merilä, P., Ostonen, I., Bengtson, P., 2022. Microbial carbon use efficiency and priming of soil organic matter mineralization by glucose additions in boreal forest soils with different C: N ratios. Soil Biol Biochem 167, 108615. https://doi.org/10.1016/j.soilbio.2022.108615.

Kirkby, C.A., Kirkegaard, J.A., Richardson, A.E., Wade, L.J., Blanchard, C., Batten, G., 2011. Stable soil organic matter: A comparison of C:N:P: S ratios in Australian and other world soils. Geoderma 163, 197–208. https://doi.org/10.1016/j.geoderma.2011.04.010.

Kuzyakov, Y., 2010. Priming effects: Interactions between living and dead organic matter. Soil Biol Biochem 42, 1363–1371. https://doi.org/10.1016/j.soilbio.2010.04.003.

Kuzyakov, Y., Friedel, J.K., Stahr, K., 2000. Review of mechanisms and quantification of priming effects. Soil Biol Biochem 32, 1485–1498. https://doi.org/10.1016/S0038-0717(00)00084-5.

Lavahun, M.F.E., Joergensen, R.G., Meyer, B., 1996. Activity and biomass of soil microorganisms at different depths. Biol Fertil Soils 23, 38–42. https://doi.org/10.1007/BF00335816.

Li, J., Pei, J., Dijkstra, F.A., Nie, M., Pendall, E., 2021a. Microbial carbon use efficiency, biomass residence time and temperature sensitivity across ecosystems and soil depths. Soil Biol Biochem 154, 108117. https://doi.org/10.1016/j.soilbio.2020.108117.

Li, J., Sang, C., Yang, J., Qu, L., Xia, Z., Sun, H., Jiang, P., Wang, X., He, H., Wang, C., 2021b. Stoichiometric imbalance and microbial community regulate microbial elements use efficiencies under nitrogen addition. Soil Biol Biochem 156, 108207. https://doi.org/10.1016/j.soilbio.2021.108207.

Liang, C., 2020. Soil microbial carbon pump: Mechanism and appraisal. Soil Ecol Lett 2, 241–254. https://doi.org/10.1007/s42832-020-0052-4.

Liao, C., Long, C., Zhang, Q., Cheng, X., 2022. Stronger effect of litter quality than micro-organisms on leaf and root litter C and N loss at different decomposition stages following a subtropical land use change. Funct Ecol 36, 896–907. https://doi.org/10.1111/1365-2435.13999.

Lin, D., Dou, P., Yang, G., Qian, S., Wang, H., Zhao, L., Yang, Y., Mi, X., Ma, K., Fanin, N., 2020. Home-field advantage of litter decomposition differs between leaves and fine roots. New Phytol nph.16517. https://doi.org/10.1111/nph.16517.

Liu, J., Chen, J., Chen, G., Guo, J., Li, Y., 2020a. Enzyme stoichiometry indicates the variation of microbial nutrient requirements at different soil depths in subtropical forests. PLOS ONE 15, e0220599.

Liu, M., Qiao, N., Xu, X., Fang, H., Wang, H., Kuzyakov, Y., 2020b. C: N stoichiometry of stable and labile organic compounds determine priming patterns. Geoderma 362, 114122. https://doi.org/10.1016/j.geoderma.2019.114122.

Maharjan, M., Sanaullah, M., Razavi, B.S., Kuzyakov, Y., 2017. Effect of land use and management practices on microbial biomass and enzyme activities in subtropical top-and sub-soils. Appl Soil Ecol 113, 22–28. https://doi.org/10.1016/j.apsoil.2017.01.008.

Manzoni, S., Taylor, P., Richter, A., Porporato, A., Ågren, G.I., 2012. Environmental and stoichiometric controls on microbial carbon-use efficiency in soils. New Phytol 196, 79–91. https://doi.org/10.1111/j.1469-8137.2012.04225.x.

Marx, M., Buegger, F., Gattinger, A., Zsolnay, Á., Charles Munch, J., 2010. Determination of the fate of regularly applied 13C-labeled-artificial-exudates C in two agricultural soils. J Plant Nutr Soil Sci 173, 80–87. https://doi.org/10.1002/jpln.200800104.

Meyer, N., Welp, G., Rodionov, A., Borchard, N., Martius, C., Amelung, W., 2018. Nitrogen and phosphorus supply controls soil organic carbon mineralization in tropical topsoil and subsoil. Soil Biol Biochem 119, 152–161. https://doi.org/10.1016/j.soilbio.2018.01.024.

Moorhead, D., Cui, Y., Sinsabaugh, R., Schimel, J., 2023. Interpreting patterns of ecoenzymatic stoichiometry. Soil Biol Biochem 180, 108997. https://doi.org/10.1016/j.soilbio.2023.108997.

Mooshammer, M., Wanek, W., Hämmerle, I., Fuchslueger, L., Hofhansl, F., Knoltsch, A., Schnecker, J., Takriti, M., Watzka, M., Wild, B., Keiblinger, K.M., Zechmeister-Boltenstern, S., Richter, A., 2014a. Adjustment of microbial nitrogen use efficiency to carbon:nitrogen imbalances regulates soil nitrogen cycling. Nat Commun 5, 3694. https://doi.org/10.1038/ncomms4694.

Mooshammer, M., Wanek, W., Zechmeister-Boltenstern, S., Richter, A., 2014b. Stoichiometric imbalances between terrestrial decomposer communities and their resources: mechanisms and implications of microbial adaptations to their resources. Front Microbiol 5.

Moreira, B.C., Prates Júnior, P., Dell, B., Kasuya, M.C.M., 2022. Roots and Beneficial Interactions with Soil Microbes. In: de Oliveira, T.S., Bell, R.W. (Eds.), Subsoil Constraints for Crop Production. Springer International Publishing, Cham, pp. 263–287.

Mori, T., 2020. Does ecoenzymatic stoichiometry really determine microbial nutrient limitations? Soil Biol Biochem 146, 107816. https://doi.org/10.1016/j.soilbio.2020.107816.

Müller, K., Kramer, S., Haslwimmer, H., Marhan, S., Scheunemann, N., Butenschön, O., Scheu, S., Kandeler, E., 2016. Carbon transfer from maize roots and litter into bacteria and fungi depends on soil depth and time. Soil Biol Biochem 93, 79–89. https://doi.org/10.1016/j.soilbio.2015.10.015.

Ning, Q., Hättenschwiler, S., Lü, X., Kardol, P., Zhang, Y., Wei, C., Xu, C., Huang, J., Li, A., Yang, J., Wang, J., Peng, Y., Peñuelas, J., Sardans, J., He, J., Xu, Z., Gao, Y., Han, X., 2021. Carbon limitation overrides acidification in mediating soil microbial activity to nitrogen enrichment in a temperate grassland. Glob Change Biol 27, 5976–5988. https://doi.org/10.1111/gcb.15819.

Ojeda, J.J., Caviglia, O.P., Agnusdei, M.G., 2018. Vertical distribution of root biomass and soil carbon stocks in forage cropping systems. Plant Soil 423, 175–191. https://doi.org/10.1007/s11104-017-3502-8.

Olsen, S.R., 1954. Estimation of Available Phosphorus in Soils by Extraction with Sodium Bicarbonate. U.S, Department of Agriculture.

Peixoto, L., Elsgaard, L., Rasmussen, J., Olesen, J.E., 2021. Nitrogen and phosphorus co-limit mineralization of labile carbon in deep subsoil. Eur J Soil Sci 72, 1879–1884. https://doi.org/10.1111/ejss.13083.

Perveen, N., Barot, S., Maire, V., Cotrufo, M.F., Shahzad, T., Blagodatskaya, E., Stewart, C.E., Ding, W., Siddiq, M.R., Dimassi, B., Mary, B., Fontaine, S., 2019. Universality of priming effect: An analysis using thirty five soils with contrasted properties sampled from five continents. Soil Biol Biochem 134, 162–171. https://doi.org/10.1016/j.soilbio.2019.03.027.

Piotrowska-Długosz, A., Długosz, J., Frąc, M., Gryta, A., Breza-Boruta, B., 2022a. Enzymatic activity and functional diversity of soil microorganisms along the soil profile – A matter of soil depth and soil-forming processes. Geoderma 416, 115779. https://doi.org/10.1016/j.geoderma.2022.115779.

Piotrowska-Długosz, A., Długosz, J., Gryta, A., Frąc, M., 2022b. Responses of N-Cycling Enzyme Activities and Functional Diversity of Soil Microorganisms to Soil Depth. Pedogenic Processes and Cultivated Plants. Agronomy 12, 264. https://doi.org/10.3390/agronomy12020264.

Pries, C.E.H., Sulman, B.N., West, C., O'Neill, C., Poppleton, E., Porras, R.C., Castanha, C., Zhu, B., Wiedemeier, D.B., Torn, M.S., 2018. Root litter decomposition slows with soil depth. Soil Biol Biochem 125, 103–114. https://doi.org/10.1016/j.soilbio.2018.07.002.

Razanamalala, K., Fanomezana, R.A., Razafimbelo, T., Chevallier, T., Trap, J., Blanchart, E., Bernard, L., 2018. The priming effect generated by stoichiometric decomposition and nutrient mining in cultivated tropical soils: Actors and drivers. Appl Soil Ecol 126, 21–33. https://doi.org/10.1016/j.apsoil.2018.02.008.

Rumpel, C., Chabbi, A., Marschner, B., 2012. Carbon Storage and Sequestration in Subsoil Horizons: Knowledge, Gaps and Potentials. In: Lal, R., Lorenz, K., Hüttl, R.F., Schneider, B.U., von Braun, J. (Eds.), Recarbonization of the Biosphere: Ecosystems and the Global Carbon Cycle. Springer, Netherlands, Dordrecht, pp. 445–464.

Rumpel, C., Kögel-Knabner, I., 2011. Deep soil organic matter—a key but poorly understood component of terrestrial C cycle. Plant Soil 338, 143–158. https://doi.org/10.1007/s11104-010-0391-5.

Salomé, C., Nunan, N., Pouteau, V., Lerch, T.Z., Chenu, C., 2010. Carbon dynamics in topsoil and in subsoil may be controlled by different regulatory mechanisms. Glob Change Biol 16, 416–426. https://doi.org/10.1111/j.1365-2486.2009.01884.x.

Sanaullah, M., Chabbi, A., Leifeld, J., Bardoux, G., Billou, D., Rumpel, C., 2011. Decomposition and stabilization of root litter in top- and subsoil horizons: what is the difference? Plant Soil 338, 127–141. https://doi.org/10.1007/s11104-010-0554-4.

Sanaullah, M., Chabbi, A., Maron, P.-A., Baumann, K., Tardy, V., Blagodatskaya, E., Kuzyakov, Y., Rumpel, C., 2016. How do microbial communities in top- and subsoil respond to root litter addition under field conditions? Soil Biol Biochem 103, 28–38. https://doi.org/10.1016/j.soilbio.2016.07.017.

Sauvadet, M., Lashermes, G., Alavoine, G., Recous, S., Chauvat, M., Maron, P.-A., Bertrand, I., 2018. High carbon use efficiency and low priming effect promote soil C stabilization under reduced tillage. Soil Biol Biochem 123, 64–73. https://doi.org/10.1016/j.soilbio.2018.04.026.

Schiedung, M., Don, A., Beare, M.H., Abiven, S., 2023. Soil carbon losses due to priming moderated by adaptation and legacy effects. Nat Geosci 16, 909–914. https://doi.org/10.1038/s41561-023-01275-3.

Schneider, F., Amelung, W., Don, A., 2021. Origin of carbon in agricultural soil profiles deduced from depth gradients of C: N ratios, carbon fractions, δ13C and δ15N values. Plant Soil 460, 123–148. https://doi.org/10.1007/s11104-020-04769-w.

Shahzad, T., Anwar, F., Hussain, S., Mahmood, F., Arif, M.S., Sahar, A., Nawaz, M.F., Perveen, N., Sanaullah, M., Rehman, K., Rashid, M.I., 2019. Carbon dynamics in surface and deep soil in response to increasing litter addition rates in an agro-ecosystem. Geoderma 333, 1–9. https://doi.org/10.1016/j.geoderma.2018.07.018.

Siegwart, L., Bertrand, I., Roupsard, O., Duthoit, M., Jourdan, C., 2022a. Root litter decomposition in a sub-Sahelian agroforestry parkland dominated by Faidherbia albida. J Arid Environ 198, 104696. https://doi.org/10.1016/j.jaridenv.2021.104696.

Siegwart, L., Jourdan, C., Piton, G., Sugihara, S., Van den Meersche, K., Bertrand, I., 2022b. Root distribution and properties of a young alley-cropping system: effects on soil carbon storage and microbial activity. Plant Soil. https://doi.org/10.1007/s11104-022-05714-9.

Siles, J.A., Díaz-López, M., Vera, A., Eisenhauer, N., Guerra, C.A., Smith, L.C., Buscot, F., Reitz, T., Breitkreuz, C., van den Hoogen, J., Crowther, T.W., Orgiazzi, A., Kuzyakov, Y., Delgado-Baquerizo, M., Bastida, F., 2022. Priming effects in soils across Europe. Glob Change Biol 28, 2146–2157. https://doi.org/10.1111/gcb.16062.

Sinsabaugh, R.L., Lauber, C.L., Weintraub, M.N., Ahmed, B., Allison, S.D., Crenshaw, C., Contosta, A.R., Cusack, D., Frey, S., Gallo, M.E., Gartner, T.B., Hobbie, S.E., Holland, K., Keeler, B.L., Powers, J.S., Stursova, M., Takacs-Vesbach, C., Waldrop, M.P., Wallenstein, M.D., Zak, D.R., Zeglin, L.H., 2008. Stoichiometry of soil enzyme activity at global scale. Ecol Lett 11, 1252–1264. https://doi.org/10.1111/j.1461-0248.2008.01245.x.

Sinsabaugh, R.L., Manzoni, S., Moorhead, D.L., Richter, A., 2013. Carbon use efficiency of microbial communities: stoichiometry, methodology and modelling. Ecol Lett 16, 930–939. https://doi.org/10.1111/ele.12113.

Song, M., Yu, L., Fu, S., Korpelainen, H., Li, C., 2020. Stoichiometric flexibility and soil bacterial communities respond to nitrogen fertilization and neighbor competition at the early stage of primary succession. Biol Fertil Soils 56, 1121–1135. https://doi.org/10.1007/s00374-020-01495-4.

Soong, J.L., Fuchslueger, L., Marañon-Jimenez, S., Torn, M.S., Janssens, I.A., Penuelas, J., Richter, A., 2020. Microbial carbon limitation: The need for integrating microorganisms into our understanding of ecosystem carbon cycling. Glob Change Biol 26, 1953–1961. https://doi.org/10.1111/gcb.14962.

Spohn, M., Klaus, K., Wanek, W., Richter, A., 2016. Microbial carbon use efficiency and biomass turnover times depending on soil depth – Implications for carbon cycling. Soil Biol Biochem 96, 74–81. https://doi.org/10.1016/j.soilbio.2016.01.016.

Tian, Q., Yang, X., Wang, X., Liao, C., Li, Q., Wang, M., Wu, Y., Liu, F., 2016. Microbial community mediated response of organic carbon mineralization to labile carbon and nitrogen addition in topsoil and subsoil. Biogeochemistry 128, 125–139. https://doi.org/10.1007/s10533-016-0198-4.

Vance, E.D., Brookes, P.C., Jenkinson, D.S., 1987a. An extraction method for measuring soil microbial biomass C. Soil Biol Biochem 19, 703–707. https://doi.org/10.1016/0038-0717(87)90052-6.

Vance, E.D., Brookes, P.C., Jenkinson, D.S., 1987b. Microbial biomass measurements in forest soils: Determination of kC values and tests of hypotheses to explain the failure of the chloroform fumigation-incubation method in acid soils. Soil Biol Biochem 19, 689–696. https://doi.org/10.1016/0038-0717(87)90050-2.

Wu, J., Brookes, P.C., Jenkinson, D.S., 1993. Formation and destruction of microbial biomass during the decomposition of glucose and ryegrass in soil. Soil Biol Biochem 25, 1435–1441. https://doi.org/10.1016/0038-0717(93)90058-J.

Xiang, S.-R., Doyle, A., Holden, P.A., Schimel, J.P., 2008. Drying and rewetting effects on C and N mineralization and microbial activity in surface and subsurface California grassland soils. Soil Biol Biochem 40, 2281–2289. https://doi.org/10.1016/j.soilbio.2008.05.004.

Zechmeister-Boltenstern, S., Keiblinger, K.M., Mooshammer, M., Peñuelas, J., Richter, A., Sardans, J., Wanek, W., 2015. The application of ecological stoichiometry to plant–microbial–soil organic matter transformations. Ecol Monogr 85, 133–155. https://doi.org/10.1890/14-0777.1.

Zhao, Y., Liang, C., Shao, S., Chen, J., Qin, H., Xu, Q., 2021. Linkages of litter and soil C: N: P stoichiometry with soil microbial resource limitation and community structure in a subtropical broadleaf forest invaded by Moso bamboo. Plant Soil 465, 473–490. https://doi.org/10.1007/s11104-021-05028-2.